ACS APPLIED MATERIALS & INTERFACES

Research Article

www.acsami.org

# Reliability Enhancement of Germanium Nanowires Using Graphene as a Protective Layer: Aspect of Thermal Stability

Jae-Hyun Lee,[†,‡] Soon-Hyung Choi,[†,‡] Shashikant P. Patole,[†] Yamujin Jang,[†,‡] Keun Heo,[‡] Won-Jae Joo,[‡] Ji-Beom Yoo,[†] Sung Woo Hwang,[‡] and Dongmok Whang*[,†,‡]

[†]SKKU Advanced Institute of Nanotechnology, School of Advanced Materials Science and Engineering, Sungkyunkwan University, Suwon 440-746, Korea

[‡]Research Center for Time-domain Nano-functional Devices, Samsung Advanced Institute of Technology, Yongin 449-712, Korea

Supporting Information

**ABSTRACT:** We synthesized thermally stable graphene-covered Ge (Ge@G) nanowires and applied them in field emission devices. Vertically aligned Ge@G nanowires were prepared by sequential growth of the Ge nanowires and graphene shells in a single chamber. As a result of the thermal treatment experiments, Ge@G nanowires were much more stable than pure Ge nanowires, maintaining their shape at high temperatures up to 850 °C. In addition, field emission devices based on the Ge@G nanowires clearly exhibited enhanced thermal reliability. Moreover, field emission characteristics yielded the highest field enhancement factor (~2298) yet reported for this type of device, and also had low turn-on voltage. Our proposed approach for the application of graphene as a protective layer for a semiconductor nanowire is an efficient way to enhance the thermal reliability of nanomaterials.

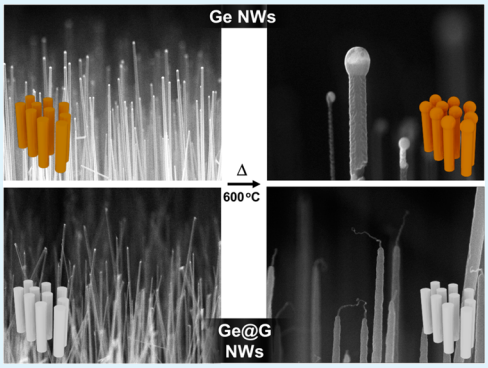


**KEYWORDS:** *germanium nanowire, graphene, core–shell, field emission, chemical vapor deposition*

## 1. INTRODUCTION

Ge nanowires (NWs) have received attention as strong candidate materials for nanoscale electronic and photonic devices, because Ge NWs have the advantages over Si NWs of higher carrier mobility and lower growth temperatures.[1−4] However, there is an obstacle of chemical instability to deal with in developing the Ge nanomaterials: their usual covering of Ge oxide is water-soluble.[5,6] Moreover, the high surface-to-volume ratio of Ge NWs makes them unstable, depressing the melting point.[7] Therefore, researchers have tried to reduce the chemical and thermal instability through various passivation approaches.[5,6,8−13] For example, the surface as-grown Ge NWs were modified by organic self-assembled molecules (SAMs).[6,8,13] SAM-coated Ge NWs are stable in the air for more than 1 week.[6,13] These SAM approaches are quite simple and cheap; however, the organic residues bring about contamination issues for electrical applications. In addition, organic layers cannot endure at high temperatures well. Accordingly, a different passivation approach, depositing stable semiconductor shells on the surface of the Ge NWs, has been suggested.[14−16] Si and SiGe alloy shells have both been successful in protecting Ge cores, and Ge/Si and Ge/SiGe core/shell NWs are suitable for use in various electronic devices, such as high-performance field-effect transistors and optoelectronics.[15,16] However, it is not easy to control the thickness of the shells, and they tend to have misfit structures due to the lattice mismatch. A third method is to deposit a carbon shell on the Ge surface.[9−12,17] By flowing a carbon-containing Ge source gas at high temperature, a Ge/C core/shell nanostructure can be obtained. The clasped carbon shell protects the core Ge from mechanical force and chemical reaction.[12,17] However, these approaches are unable to control the diameter or length of the Ge NWs, or the thickness of the carbon sheath.[9−11] Furthermore, the carbon-coating process deformed the Ge NWs structures by exposing them to high temperatures for a long time.[17]

To increase the functionality of the shell protecting the Ge surface, it should (i) be highly stable, both chemically and physically; (ii) be very thin; and (iii) be easily removable. Graphene can meet all of these requirements. Graphene has been extensively studied in various fields.[18−24] Especially, it has been used as a protecting layer for metals because of its perfect honeycomb structures with strong $sp^2$ hybridization; graphene efficiently suppresses corrosion and oxidation of the underlying metals, reducing the rate of these reactions by a factor of 10 or more compared to those for the bare metals.[25,26] Recently, Kim et al. successfully demonstrated that graphene shells preserve Ge NWs from mechanical stresses during lithiation/delithiation cycles.[27] However, there have been no reports on the use of graphene to enhance the thermal stability of nanomaterials.

Herein, we confirmed the possibility of using a graphene layer to protect semiconductor Ge NWs from thermal energy.

Received: January 11, 2014
Accepted: March 11, 2014
Published: March 11, 2014

   dx.doi.org/10.1021/am5001294 | ACS Appl. Mater. Interfaces 2014, 6, 5069−5074

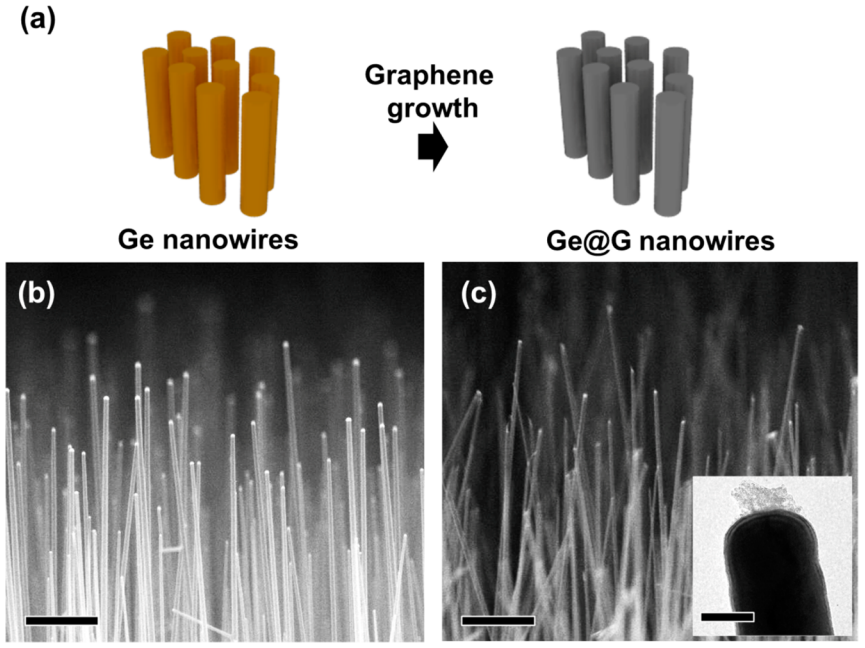


**Figure 1.** (a) Schematic illustration of Ge@G NW growth. Cross-sectional SEM images of vertically grown (b) Ge NWs and (c) Ge@G NWs; scale bar: 1 $\mu$m. Inset of (c) shows HR-TEM image of the top region of the Ge@G NWs; scale bar: 50 nm.

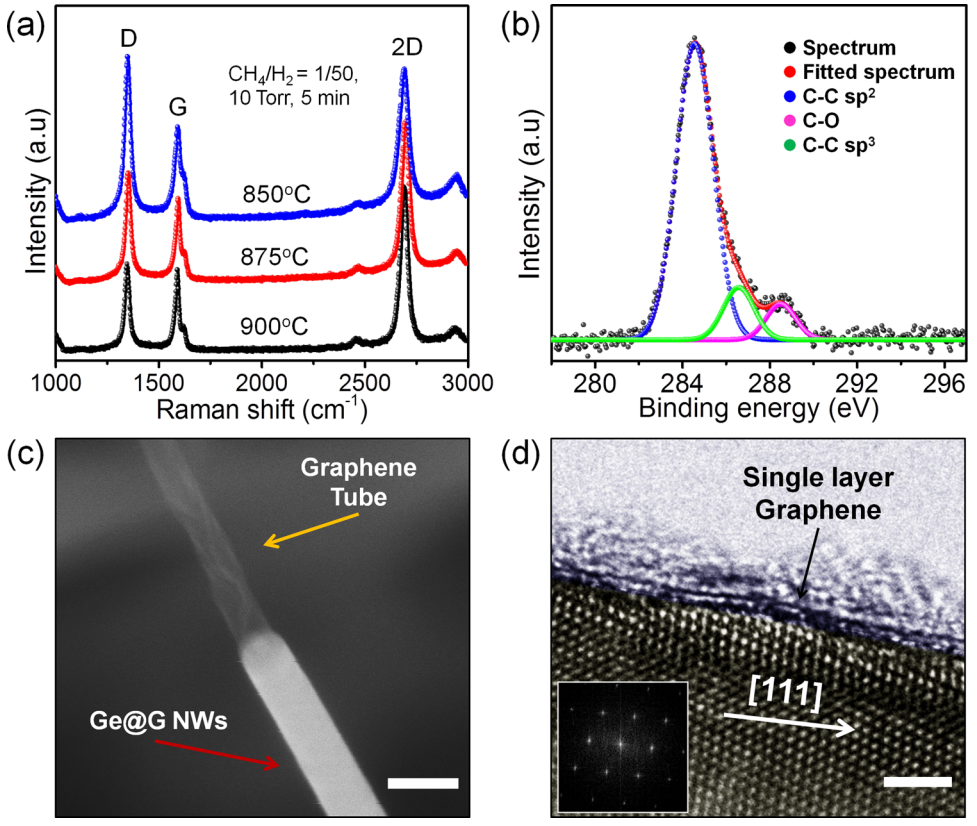


**Figure 2.** (a) Raman spectra of Ge@G NWs. Three specific peaks are located ranging from 1300 to 3200 cm$^{-1}$. (b) XPS spectra of Ge@G NWs. (c) SEM image of graphene nanotube−Ge@G NW hybrid structures after thermal annealing of Ge@G NWs in vacuum for 10 min at 800 °C; scale bar: 100 nm. (d) HR-TEM image of the Ge core and graphene shell. Single-layer graphene covers the surface of Ge NWs; scale bar: 2 nm. Inset shows a SAED pattern from Ge@G NW.

Ge is an effective catalyst for single-layer graphene growth because of the extremely low solid solubility of C in Ge.[27,28] We describe our synthesis of graphene-covered Ge NWs (Ge@G NWs) using a conventional low-pressure chemical vapor deposition (LPCVD) system; these Ge@G NWs exhibited high thermal stability and maintained their original NW structures at 850 °C. We also applied Ge@G NWs in field emission devices to compare the thermal reliability of these


dx.doi.org/10.1021/am5001294 | ACS Appl. Mater. Interfaces 2014, 6, 5069−5074

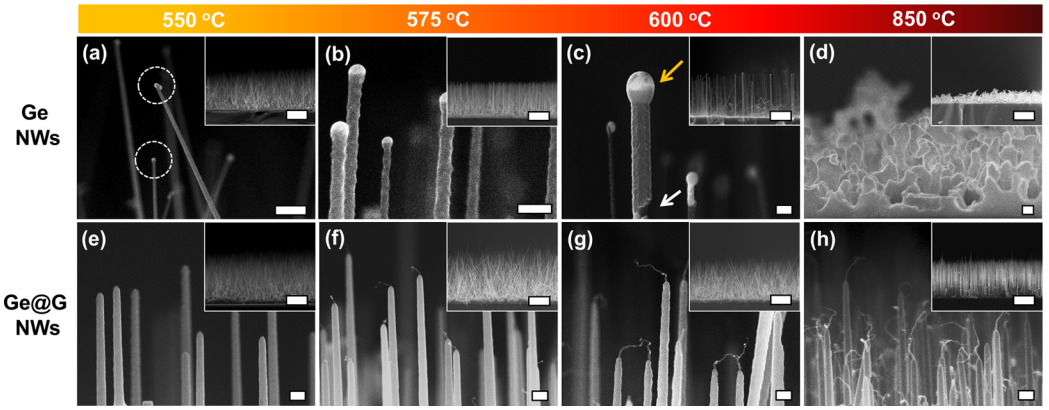


**Figure 3.** Comparison of thermal stability of pure Ge NWs and Ge@G NWs. (a–d) Cross-sectional images of pure Ge NWs after thermal annealing in vacuum for 10 min at (a) 550, (b) 575, (c) 600, and (d) 850 °C; scale bar: 200 nm. Insets show low-magnification images of the Ge NWs. At 600 °C, the density of the pure Ge NWs is significantly decreased. At 850 °C; scale bar: 1 $\mu$m. (e–h) Cross-sectional images of Ge@G NWs after thermal annealing in vacuum for 10 min at (e) 550, (f) 575, (g) 600, and (h) 850 °C; scale bar: 200 nm. Insets show low-magnification images of the Ge@G NWs. There were no noticeable differences in density among the Ge@G NWs in this temperature range; scale bar: 1 $\mu$m.

devices when the graphene-covered and pure Ge NWs were used. The field emission characteristics of the device based on Ge@G NWs exhibited the highest field enhancement factor (~2298) yet reported for this type of device.

## 2. EXPERIEMENTAL DETAILS

**Synthesis of Vertically Aligned Ge@G NWs.** Three nm thickness Au films were deposited on H-terminated Si(111) wafers by thermal evaporation. The substrate was loaded in an LPCVD system, and the chamber was evacuated. The furnace was then heated to 420 °C under an Ar atmosphere with a base pressure of 5 mTorr. $GeH_4$ (20 sccm, 10% diluted in $H_2$) was flowed as a Ge source at 420 °C and 10 Torr for 20 min. To prevent unwanted deposition of Ge during the NW growth, we added HCl gas (5 sccm, 50% diluted in $N_2$). The graphene shell on the Ge NW was grown in the same chamber. After growth of Ge NWs, the furnace was heated up to 850–900 °C; simultaneously, a mixture of $CH_4$ and $H_2$ ($CH_4$:$H_2$ ratio of 1:50) gas was flowed for 5 min with maintaining a total pressure of 10 Torr.

**Characterization.** SEM images were measured using a JEOL JSM-7401F field emission scanning electron microscope. The crystallinity and composition of the NWs were characterized using a JEOL ARM 200F and a JEM-2100F transmission electron microscope (TEM). For TEM imaging, Ge NWs and Ge@G NWs were suspended in ethanol, dispersed onto a Cu grid without a lacey carbon support film, and imaged at an accelerating voltage of 80 and 200 kV. XPS analysis was carried out in an ESCA2000 spectrometer using monochromatic Al K$\alpha$ radiation (1468.6 eV). The peak energies were calibrated to the C 1s peak at 284.6 eV. Raman spectroscopy (Renishaw, RM-1000 Invia) with an excitation energy of 2.41 eV (514 nm; Ar ion laser) was used to characterize NWs of both types dispersed on 300 nm $SiO_2$ substrates. Current–voltage ($I_{ds}$–$V_{ds}$) and transfer ($I_{ds}$–$V_g$) characteristics of single graphene nanoribborn (GNR) devices were measured using a Keithley 4200 SCS at room temperature.

**Field Emission Measurement.** The field emission characteristics of the as-grown samples were measured in a high-vacuum chamber with a parallel diode type configuration at a base pressure of $10^{-7}$ Torr. The FE current was measured at different voltages using an automatically controlled Keithley 2001 electrometer and power supply (Fug Power HCN 700-3500).

## 3. RESULTS AND DISCUSSION

The in-situ growth process used to vertically grow Ge@G NWs on a Si(111) substrate is shown schematically in Figure 1a. We first grew epitaxial Ge NWs on a Si(111) substrate via previously reported methods.[29] The graphene protective shell was grown immediately thereafter at 850 °C. After the growth of the graphene shell, the tip region of the NWs was slightly melted and evaporated while the vertical structure of the Ge@G NWs was well-preserved (Figure 1b,c). The HR-TEM image of the Ge@G NW clearly shows that the crumpled graphene was grown on the tip of the NWs (inset of Figure 1c). In contrast, when pure Ge NWs were exposed to vacuum for 5 min at 850 °C without supply of the carbon source to form the graphene shell, they were completely melted, forming polycrystalline Ge film (Figure S1, Supporting Information).

The growth of the graphene shell on Ge NWs was confirmed by various spectroscopy and microscopy tools. Three specific peaks, the D band, G band, and 2D band, are observed in the Raman spectrum at ~1345, ~1588, and ~2688 $cm^{-1}$, respectively; this is strong evidence of the existence of a graphene shell (Figure 2a).[30] The intensity of the D peak is a good indicator that confirms the quality of graphene.[30,31] When the graphene shell is grown at 850 °C, the intensity ratio of $I(D)/I(G)$ is over 1.3, and this ratio decreases as the growth temperature increases. These results indicated that the quality of graphene strongly depends on the growth temperature. However, if the growth temperature was over 850 °C, the vertically aligned structure of Ge NWs was severely deformed (Figure S2, Supporting Information). We also measured the transmittance by using an ultraviolet–visible spectrometer, after transferring the graphene on the quartz (Figure S3, Supporting Information). Ge-catalyzed graphene shows high transmittance over 97.5% at the visible range, which is comparable to the value of the absorption of single-layer graphene.[32] The Raman peak at ~300 $cm^{-1}$ and its full width at half-maximum indicate that the crystallinity of the Ge NWs is not affected by high temperatures after graphene growth (Figure S4, Supporting Information). X-ray photoelectron spectroscopy (XPS) was employed to investigate the chemical state of the graphene shell; a peak at 284.6 eV corresponded to the C–C bond of $sp^2$ carbon, while a peak at 288.7 eV corresponded to C=O groups (Figure 2b). In the XPS spectrum, the intensity of the C–C bond was almost 97%, confirming that the dominant state of the graphene shells was $sp^2$-hybridized carbon. To see the graphene shell more clearly, Ge@G NWs were annealed in vacuum for 10 min at 800 °C. Figure 2c shows thin and uniform graphene nanotubes connected to the Ge@G NWs because of the Ge evaporation. HR-TEM analysis of the Ge@G


dx.doi.org/10.1021/am5001294 | ACS Appl. Mater. Interfaces 2014, 6, 5069–5074

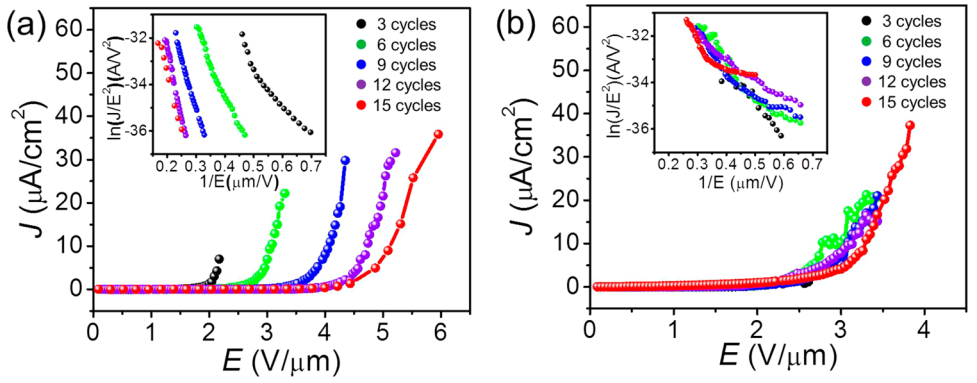


**Figure 4.** Field emission results of (a) pure GeNWs and (b) Ge@G NWs. (Insets) FN plots of both FE results.

**Table 1. Summary of Turn-On Voltages and FEFs of Ge NWs and Ge@G NWs**

| number of cycles | | 3 | 6 | 9 | 12 | 15 |
|---|---|---|---|---|---|---|
| Ge NWs | turn-on voltage [V $\mu m^{-1}$] | 1.9 | 2.6 | 3.4 | 4.1 | 4.3 |
| | FEF ($\beta$) | 1817.5 | 1308.8 | 805.1 | 619.1 | 687.1 |
| Ge@G NWs | turn-on voltage [V $\mu m^{-1}$] | 2.4 | 2.4 | 2.3 | 2.1 | 2.0 |
| | FEF ($\beta$) | 2214.7 | 2190.4 | 2083.2 | 2298.7 | 1953.9 |
| reference results | turn-on voltage [V $\mu m^{-1}$] | | 7.6[35] | 4.6[39] | 15[40] | |
| | FEF ($\beta$) | | 505.9[35] | 1242[39] | 560[40] | |

NWs indicated that a single layer of graphene covered the Ge NWs (Figure 2d). XPS and TEM results of both pure Ge NWs and Ge@G NWs after 1 week exposure in air show that the graphene shell efficiently suppresses the surface oxidation of Ge NWs, although the surface oxidation was not completely blocked because of the structural defects of the single-layered graphene shell (Figure S5, Supporting Information). Furthermore, to investigate the electrical properties of the graphene shell, we fabricated a single graphene nanoribbon (GNR) field effect transistor (FET). The GNR device showed p-type behavior, which is a conventional property of GNRs (Figures S6 and S7, Supporting Information).[33,34]

Previous studies have shown that a graphitic or other carbon shell can enhance the chemical or physical stability of Ge NWs.[12,17,24,27] For example, a simultaneously grown carbon shell prevents oxidation of Ge NWs.[12] Moreover, Ge NWs coated with carbon sheaths have been used for an anode material of a highly reproducible lithium-ion battery.[17,27] However, there is no research on the thermal stability of NWs. In our studies, we test thermal stability by attempting to anneal the Ge NWs and Ge@G NWs in the vacuum at high temperature. Figure 3 shows SEM images of Ge NWs and Ge@G NWs after thermal annealing at various temperatures. Pure Ge NWs started to melt at 550 °C (approx. 380 °C lower than the melting point of bulk Ge); the tips of the Ge NWs were melted and became slightly kinked. At 575 °C, the surfaces of the Ge NWs started to melt, inducing a wavy roughness. At 600 °C, the small-diameter Ge NWs were completely melted and only large-diameter Ge NWs remained. The tips of the large-diameter Ge NWs were spherical, and their surfaces were very rough due to surface melting and evaporation. Finally, Ge NWs were completely melted at 850 °C. On the contrary, Ge@G NWs maintained their 1D structure; even the temperature reached up to 850 °C. Interestingly, we can find the continuous growth of graphene nanotubes on top of Ge@G NWs as the temperature increased. It might be caused by the Ge evaporation via graphene nanotubes. The main reason for this difference in melting points is strongly related to their surface energy.[7,35−37] For a cylindrical bare nanowire with a radius $r$ and length $L$, the surface energy is given by[36] $\sigma S(r) = 2\sigma V(r^{-1} + L^{-1})$, where $\sigma$ is the surface energy or surface tension per unit area, $S(r)$ is the surface area of the nanowire, and $V$ is the volume. When the size is decreased to the nanometer scale, the surface-to-volume ratio increases greatly, along with the surface curvature, and surface energy dominates the overall thermal stability. The strong $sp^2$-hybridized graphene shell decreases not only the surface energy but also the interface energy between Ge and graphene. On the contrary, the surface of a pure Ge NW is covered by a thin and unstable $GeO_x$ layer.[5,6] Generally, $GeO_x$ layers generate large numbers of dangling bonds, thereby increasing the surface energy.[38] Therefore, though the average diameters of both NWs are similar, the Ge@G NWs are much more thermally stable than pure Ge NWs.

We adopted our pure Ge NWs and thermally stable Ge@G NWs for field emission (FE) devices. Various types of FE devices based on Ge nanostructures have been demonstrated,[35,39,40] but the use of Ge NWs formed by the vapor−liquid−solid (VLS) method in FE devices has not yet been reported. Figure 4 shows field emission characteristics of pure Ge NWs and Ge@G NWs. The VLS method is widely used to vertically grow group IV NWs.[2,12,15,29] The vertical structure of Ge NWs is the proper shape for FE applications; however, compared with other nanomaterials, it has been difficult to adopt in FE devices due to the thermal stability issue, despite its good aspect ratio and high carrier mobility.

Table 1 summarizes the turn-on voltage ($V_{on}$) and field enhancement factor (FEF) difference between FE devices based on Ge NWs and Ge@G NWs. The FE current−voltage characteristics can be expressed by a simplified Fowler−Nordheim (FN) equation

$$J = (A\beta^2E^2 2/\phi)\exp(-(B\phi^{3/2})/\beta E)$$

where $A = 1.54 \times 10^{-6}$ A eV $V^{-2}$, $B = 6.83 \times 10^3$ $eV^{-3/2}$ V $\mu m^{-1}$, and $\phi$ is the work function of the emitting materials,


dx.doi.org/10.1021/am5001294 | ACS Appl. Mater. Interfaces 2014, 6, 5069−5074

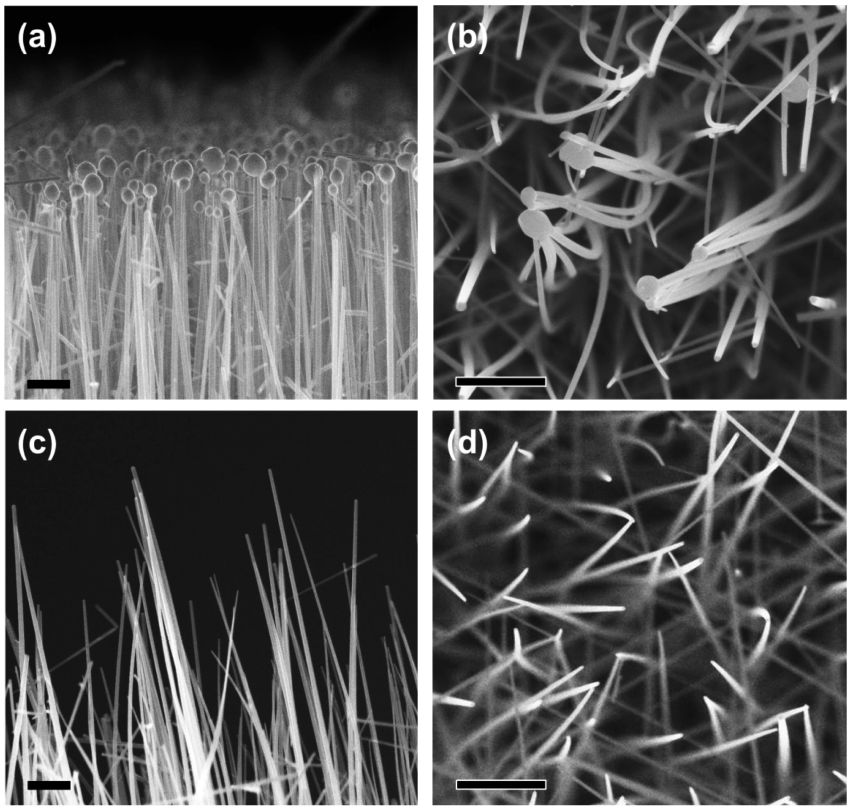


**Figure 5.** SEM images of (a, b) pure Ge NWs and (c, d) Ge@G NWs after 15 cycles of FE measurement; scale bar: 1 $\mu$m.

which is 5.15 eV for Ge. Repeated FE measurement changes the turn-on voltage of the pure Ge NWs from 1.9 to 4.3 V $\mu m^{-1}$. In contrast, the turn-on voltage of Ge@G NWs stays around 2.0−2.4 V $\mu m^{-1}$. To check the reproducibility, we measured one more device and confirmed it (Figure S8, Supporting Information). The gradually increased turn-on voltages are mainly attributed to changing shapes of the emitters, since the FEF of pure Ge NWs is significantly reduced by repeated measurements. FEF is strongly related to the geometry, crystallinity, and density of emitters.[35,41] The FEF of pure Ge NW FE devices significantly decreased, but that of the devices based on Ge@G NWs stayed around 2000, which is the highest value yet reported for Ge-based FE devices.[35,39,40] This may be due to the high aspect ratio of the NWs with a clumped and conductive graphene on the tip. Herein, the Ge@G NWs had an average length of 20 $\mu$m and an average diameter of 50−70 nm, and thus, the aspect ratio is 300−400.

SEM and TEM analyses identify the degradation of the Ge NWs after 15 cycles of FE measurement, with a change in geometry of the tips of the pure Ge NWs (Figure 5 and Figure S9, Supporting Information). Since the high voltage was focused on the sharp Ge tips, the temperature was increased with a partial melt of the NWs.[42] The tips of the NWs were melted, forming Ge nanospheres and thereby reducing their surface energy. Selected area electron diffraction (SAED) patterns indicated that two single-crystalline Ge NWs were welded at the top region of the NWs (Figure S9, Supporting Information). In comparison, Ge@G NWs show no surface melting phenomena (Figure 5c,d).

## 4. CONCLUSION

We synthesized Ge@G NWs with enhanced thermal reliability using an in-situ growth method. In contrast with pure Ge NWs, Ge@G NWs maintained their original structure at high temperature because the protective graphene shells mitigated the nanoscale phenomenon of melting point depression. In addition, we applied Ge@G NWs in FE devices, where they showed higher stability compared to devices based on Ge NWs. Our approach may provide an efficient way to enhance the stability of nanomaterials.

## ■ ASSOCIATED CONTENT

### Supporting Information

Graphene shell effects; SEM images of Ge@G NWs after annealing process and field emission measurement; scheme for single-GNR device fabrications; and $I_{ds}$−$V_{ds}$ characteristics of Ge@G NWs and GNR. This material is available free of charge via the Internet at http://pubs.acs.org.

## ■ AUTHOR INFORMATION

### Corresponding Author

*E-mail: dwhang@skku.edu.

### Notes

The authors declare no competing financial interest.

## ■ ACKNOWLEDGMENTS

This work was supported by the National Research Foundation of Korea (NRF) grant funded by the Korea government (MSIP) (No. 2007-0054845). D.W. acknowledges support from the Basic Science Research Program through the NRF (No. 2009-0083540).

## ■ REFERENCES

(1) Sze, S. M.; Ng, K. K. *Physics of Semiconductor Devices*, 2nd ed.; Wiley: New York, 1981.

(2) Cui, Y.; Lauhon, L. J.; Gudiksen, M. S.; Wang, J.; Lieber, C. M. Diameter-controlled synthesis of single-crystal silicon nanowires. *Appl. Phys. Lett.* **2001**, *78*, 2214−2216.
(3) Wu, Y.; Yang, P. Germanium nanowire growth via simple vapor transport. *Chem. Mater.* **2000**, *12*, 605−607.
(4) Cao, L.; White, J. S.; Park, J. S.; Schuller, J. A.; Clemens, B. M.; Brongersma, M. L. Engineering light absorption in semiconductor nanowire devices. *Nat. Mater.* **2009**, *8*, 643−647.
(5) Collins, G.; Holmes, J. D. Chemical functionalisation of silicon and germanium nanowires. *J. Mater. Chem.* **2011**, *21*, 11052−11069.
(6) Wang, D.; Chang, Y. L.; Wang, Q.; Cao, J.; Farmer, D. B.; Gordon, R. G.; Dai, H. Surface chemistry and electrical properties of germanium nanowires. *J. Am. Chem. Soc.* **2004**, *126*, 11602−11611.
(7) Wu, Y.; Yang, P. Melting and welding semiconductor nanowires in nanotubes. *Adv. Mater.* **2001**, *13*, 520−523.
(8) Hanrath, T.; Korgel, B. A. Chemical surface passivation of Ge nanowires. *J. Am. Chem. Soc.* **2004**, *126*, 15466−15472.
(9) Mathur, S.; Shen, H.; Sivakov, V.; Werner, U. Germanium nanowires and core−shell nanostructures by chemical vapor deposition of $[Ge(C_5H_5)_2]$. *Chem. Mater.* **2004**, *16*, 2449−2456.
(10) Huang, Y.; Lin, J.; Zhang, J.; Ding, X. X.; Qi, S. R.; Tang, C. C. A novel method for preparing carbon-coated germanium nanowires. *Nanotechnology* **2005**, *16*, 1369−1371.
(11) Pandurangan, A.; Morin, C.; Qian, D.; Andrews, R.; Crocker, M. Single-step synthesis of germanium nanowires encapsulated within multi-walled carbon nanotubes. *Carbon* **2009**, *47*, 1708−1714.
(12) Kim, B. S.; Kim, M. J.; Lee, J. C.; Hwang, S. W.; Choi, B. L.; Lee, E. K.; Whang, D. Control of lateral dimension in metal-catalyzed germanium nanowire growth: Usage of carbon sheath. *Nano Lett.* **2012**, *12*, 4007−4012.
(13) Holmberg, V. C.; Korgel, B. A. Corrosion resistance of thiol- and alkene-passivated germanium nanowires. *Chem. Mater.* **2010**, *22*, 3698−3703.
(14) Arnold, D. C.; Hobbs, R. G.; Zirngast, M.; Marschner, C.; Hill, J. J.; Ziegler, K. J.; Morris, M. A.; Holmes, J. D. Single step synthesis of Ge−$SiO_x$ core-shell heterostructured nanowires. *J. Mater. Chem.* **2009**, *19*, 954−961.
(15) Lauhon, L. J.; Gudlksen, M. S.; Wang, D.; Lieber, C. M. Epitaxial core−shell and core−multishell nanowire heterostructures. *Nature* **2002**, *420*, 57−61.
(16) Hu, S.; Kawamura, Y.; Huang, K. C. Y.; Li, Y.; Marshall, A. F.; Itoh, K. M.; Brongersma, M. L.; McIntyre, P. C. Thermal stability and surface passivation of Ge nanowires coated by epitaxial SiGe shells. *Nano Lett.* **2012**, *12*, 1385−1391.
(17) Seo, M. H.; Park, M.; Lee, K. T.; Kim, K.; Kim, J.; Cho, J. High performance Ge nanowire anode sheathed with carbon for lithium rechargeable batteries. *Energy Environ. Sci.* **2011**, *4*, 425−428.
(18) Geim, A. K. Graphene: Status and prospects. *Science* **2009**, *324*, 1530−1534.
(19) Zhang, Y.; Tan, Y. W.; Stormer, H. L.; Kim, P. Experimental observation of the quantum Hall effect and Berry's phase in graphene. *Nature* **2005**, *438*, 201−204.
(20) Novoselov, K. S.; Geim, A. K.; Morozov, S. V.; Jiang, D.; Grigorieva, M.; Dubonos, S. V.; Firsov, A. A. Two-dimensional gas of massless Dirac fermions in graphene. *Nature* **2005**, *438*, 197−200.
(21) Huang, X.; Yin, Z.; Wu, S.; Qi, X.; He, Q.; Zhang, Q.; Yan, Q.; Boey, F.; Zhang, H. Graphene-based materials: Synthesis, characterization, properties, and applications. *Small* **2011**, *7*, 1876−1902.
(22) Kim, Y. H.; Kwon, S. H.; Lee, J. M.; Hwang, M. S.; Kang, J. H.; Park, W. I.; Park, H. G. Graphene-contact electrically driven microdisk lasers. *Nat. Commun.* **2012**, *3*, 1123.
(23) Khan, U.; May, P.; Porwal, H.; Nawaz, K.; Coleman, J. N. Improved adhesive strength and toughness of polyvinyl acetate glue on addition of small quantities of graphene. *ACS Appl. Mater. Interfaces* **2013**, *5*, 1423−1428.
(24) Zhou, W.; Zhu, J.; Cheng, C.; Liu, J.; Yang, H.; Cong, C.; Guan, C.; Jia, X.; Fan, H. J.; Yan, Q.; Li, C. M.; Yu, T. A general strategy toward graphene@metal oxide core−shell nanostructures for high-performance lithium storage. *Energy Environ. Sci.* **2011**, *4*, 4954−4961.
(25) Prasai, D.; Tuberquia, J. C.; Harl, R. R.; Jennings, G. K.; Bolotin, K. I. Graphene: Corrosion-inhibiting coating. *ACS Nano* **2012**, *6*, 1102−1108.
(26) Chen, S.; Brown, L.; Levendorf, M.; Cai, W.; Ju, S. Y.; Edgeworth, J.; Li, X.; Magnuson, C. W.; Velamakanni, A.; Piner, R. D.; Kang, J.; Park, J.; Ruoff, R. S. Oxidation resistance of graphene-coated Cu and Cu/Ni alloy. *ACS Nano* **2011**, *5*, 1321−1327.
(27) Kim, H.; Son, Y.; Park, C.; Cho, J.; Choi, H. C. Catalyst-free direct growth of a single to a few layers of graphene on a germanium nanowire for the anode material of a lithium battery. *Angew. Chem., Int. Ed.* **2013**, *52*, 5997−6001.
(28) Wang, G.; Zhang, M.; Zhu, Y.; Ding, G.; Jiang, D.; Guo, Q.; Liu, S.; Xie, X.; Chu, P. K.; Di, Z.; Wang, X. Direct growth of graphene film on germanium substrate. *Sci. Rep.* **2013**, *3*, 2465.
(29) Adhikari, H.; Marshall, A. F.; Chidsey, C. E. D.; McIntyre, P. C. Germanium nanowire epitaxy: Shape and orientation control. *Nano Lett.* **2006**, *6*, 318−323.
(30) Ferrari, A. C.; Meyer, J. C.; Scardaci, V.; Casiraghi, C.; Lazzeri, M.; Mauri, F.; Piscanec, S.; Jiang, D.; Novoselov, K. S.; Roth, S.; Geim, A. K. Raman spectrum of graphene and graphene layers. *Phys. Rev. Lett.* **2006**, *97*, 187401.
(31) Cançado, L. G.; Jorio, A.; Ferreira, E. H. M.; Stavale, F.; Achete, C. A.; Capaz, R. B.; Moutinho, M. V. O.; Lombardo, A.; Kulmala, T. S.; Ferrari, A. C. Quantifying defects in graphene via Raman spectroscopy at different excitation energies. *Nano Lett.* **2011**, *11*, 3190−3196.
(32) Nair, R. R.; Blake, P.; Grigorenko, A. N.; Novoselov, K. S.; Booth, T. J.; Stauber, T.; Peres, N. M. R.; Geim, A. K. Fine structure constant defines visual transparency of graphene. *Science* **2008**, *320*, 1308.
(33) Bai, J.; Duan, X.; Huang, Y. Rational fabrication of graphene nanoribbons using a nanowire etch mask. *Nano Lett.* **2009**, *9*, 2083−2087.
(34) Kosynkin, D. V.; Higginbotham, A. L.; Sinitskii, A.; Lomeda, J. R.; Dimiev, A.; Price, B. K.; Tour, J. M. Longitudinal unzipping of carbon nanotubes to form graphene nanoribbons. *Nature* **2009**, *458*, 872−876.
(35) Li, L.; Fang, X.; Chew, H. G.; Zheng, F.; Liew, T. H.; Xu, X.; Zhang, Y.; Pan, S.; Li, G.; Zhang, L. Crystallinity-controlled Germanium nanowire arrays: Potential field emitters. *Adv. Funct. Mater.* **2008**, *18*, 1080−1088.
(36) Zhang, Y. F.; Tang, Y. H.; Wang, N.; Lee, C. S.; Bello, I.; Lee, S. T. Germanium nanowires sheathed with an oxide layer. *Phys. Rev. B* **2000**, *61*, 4518−4521.
(37) Xu, Q.; Sharp, I. D.; Yuan, C. W.; Yi, D. O.; Liao, C. Y.; Glaeser, A. M.; Minor, A. M.; Beeman, J. W.; Ridgway, M. C.; Kluth, P.; Ager Iii, J. W.; Chrzan, D. C.; Haller, E. E. Large melting-point hysteresis of Ge nanocrystals embedded in $SiO_2$. *Phys. Rev. Lett.* **2006**, *97*, 155701.
(38) Bodlaki, D.; Yamamoto, H.; Waldeck, D. H.; Borguet, E. Ambient stability of chemically passivated germanium interfaces. *Surf. Sci.* **2003**, *543*, 63−74.
(39) Wu, H. C.; Hou, T. C.; Chueh, Y. L.; Chen, L. J.; Chiu, H. T.; Lee, C. Y. One-dimensional germanium nanostructures-formation and their electron field emission properties. *Nanotechnology* **2010**, *21*, 455601.
(40) Wan, Q.; Wang, T. H.; Feng, T.; Liu, X. H.; Lin, C. L. Synthesis of large-area germanium cone-arrays for application in electron field emission. *Appl. Phys. Lett.* **2002**, *81*, 3281−3283.
(41) Fang, X.; Bando, Y.; Gautam, U. K.; Ye, C.; Golberg, D. Inorganic semiconductor nanostructures and their field-emission applications. *J. Mater. Chem.* **2008**, *18*, 509−522.
(42) Purcell, S. T.; Vincent, P.; Journet, C.; Binh, V. T. Hot nanotubes: Stable heating of individual multiwall carbon nanotubes to 2000 K induced by the field-emission current. *Phys. Rev. Lett.* **2002**, *88*, 105502.